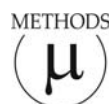


STUDIA GEOLOGICA POLONICA

Vol. 124, Kraków 2005, pp. 53–65.

Methods and Applications in Micropalaeontology

*Edited by J. Tyszka, M. Oliwkiewicz-Mikłasińska,
P. Gedl & M. A. Kaminski*



Jan BARTHOLDY¹, Thomas LEIPE², Peter FRENZEL³, Franz TAUBER²
& Rainer BAHLO²

High resolution Single Particle Analysis by scanning electron microscopy: A new tool to investigate the mineral composition of agglutinated foraminifers

(Figs 1–3; Tabs 1–6)

Abstract. A high resolution Single Particle Analysis by scanning electron microscopy (SEM) and X-ray microanalysis is introduced as a new technique to investigate components of tests of agglutinated foraminifers. In a feasibility study, specimens of *Nodulina dentaliniformis* (Brady, 1881) from surface sediment of the Lübeck Bight (southwestern Baltic Sea) were investigated. A chemical mapping of a selected part of the surface of the last chamber as well as analysis of isolated foraminiferal shell grains and the ambient sediment were carried out. The investigations point to the non-selectivity of the foraminifer to use specific minerals but a selectivity to use specific grain sizes and shapes.

Key words: X-ray microanalysis, single particle analysis, multielement mapping, agglutinated foraminifera, shell composition.

INTRODUCTION

Foraminifera are among the most abundant, diverse and widely distributed groups of protozoans in marine and brackish water environments, and have a particularly well documented fossil record. Test morphologies and compositions may be indicative for the ambient environment (e. g., Kuhnt *et al.*, 1996; Nomura, 1988). Depending on the systematic group, the shell may be made of organic compounds, particles cemented together (agglutinated), secreted in crystalline calcium carbon-

1 University of Bonn, Institute of Paleontology, Nussallee 8, 53115 Bonn, Germany. E-mail: mailto@jan-bartholdy.de

2 Institute of Baltic Sea Research, Seestrasse 5, 18119 Rostock-Warnemünde, Germany

3 University of Rostock, Institute of Aquatic Ecology, Albert-Einstein-Str. 3, 18059 Rostock, Germany

ate or in some cases in SiO₂. Traditionally, the classification of foraminifers is based primarily on the nature of their shells (Loeblich & Tappan, 1989).

Agglutinated taxa are classified by external and internal characteristics, the microstructural nature of wall, and the arrangement of components as well as the cement morphology and composition (e.g., Bender & Hemleben 1995).

The selective uptake of particles, their arrangement in the shell, and the nature of the cement are still under debate. There is an evidence for the selectivity of *Ammobaculites balkwilli* for distinct anatase grains, and some observations that certain foraminifers can select particles according to their size (Allen *et al.*, 1999). Biochemical and microprobe techniques have been used in the investigation of particle and cement composition and have been given new insights (Allen *et al.*, 1998, 1999; Mancin, 2001). Despite all investigations, many questions are still unresolved.

This paper introduces a new microprobe technique, applicable for the investigation of agglutinated foraminifera: The high resolution analysis by scanning electron microscopy provides the opportunity of analyzing surfaces or isolated grains unattended in high quantities physical (diameter, shape, perimeter, area), and chemical. Our feasibility study of investigations on *Nodulina dentaliniformis* (Brady, 1881) specimens from the Baltic Sea demonstrates the possibilities of this new technique. Specific questions in mineral composition and the selective uptake of grains are discussed.

MATERIAL AND METHODS

For this study, sediment samples from the Lübeck Bight (southwestern Baltic Sea) were taken from the sea bottom, using a multicorer device. The surface material of the first 3 cm of the core was washed over a 63 µm sieve, and dried at 40°C. Specimens of living, Rose Bengal stained, *N. dentaliniformis* were picked using a binocular. In the Baltic, this agglutinating foraminifer inhabits fine grained sediments with different contents of organic matter in depths between 16 to 44 m from the Belt Sea to the Gotland Basin (Hermelin, 1987; Lutze, 1965).

From the station no. 280000 (011°10'E, 54°06'W) at 23.5 m water depth, three samples were investigated, using the introduced technique. Two well preserved, empty specimens of *N. dentaliniformis* were selected and cleaned carefully with distilled water, using a fine brush (Fig. 1).

The first one (sample "nodulina 1") was mounted on an aluminium stub and coated with Carbon for multielement mapping. A selected area of the last chambers surface was analyzed with the "EDAX Genesis 4000" tool for the elements Al, Ca, Fe, K, Mg, Mn, Na, P, S, Si, and Ti, using a dense rectangular grid with the size 284 x 220 µm. The resulting images for individual elements have a matrix of 1024 x 800 pixels, and a spatial resolution of about 0.28 µm. The gray-scale intensities of the individual pixels are related to the concentration of the element at this point of the measured area.

The second test (sample "nodulina 2") was prepared for the single particle

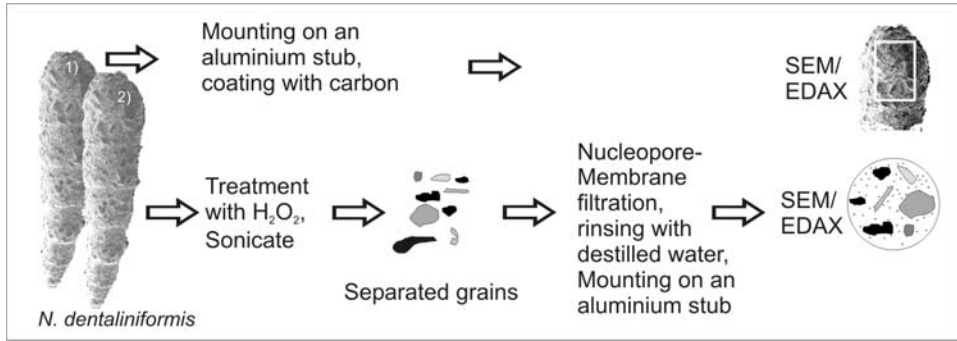


Fig. 1. Simplified description of the sample preparation for the multielement mapping (upper line), and the Single Particle Analysis respectively (lower line)

analysis. To disintegrate the shell, the shell was treated with hydrogen peroxide (H₂O₂) oxidizing the organic cement. The nature of the cement was determined separately on broken off specimens of *N. dentaliniformis* from the Luebeck Bight and the Darss Sill. After a few hours of H₂O₂ treatment, the samples were sonicated for some minutes and filtrated through a Nucleopore membrane filter. The particles of the former shell are scattered on the filter membrane which was dried at 40°C, mounted on an aluminium stub and coated with carbon for the X-ray microanalysis. Additionally, a H₂O₂ treated, homogenized sediment sample from station 280000 was prepared in the same way (sample “substrate”).

For analyzing the agglutinated shell surfaces and the isolated components of the shells, a Quanta FEI 400 electron microscope, equipped with an X-ray microanalysis EDAX GENESIS 4000, at the Baltic Sea Research Institute Warnemünde was used. The Quanta FEI 400 is a versatile high performance, low vacuum scanning electron microscope with three imaging modes (high vacuum, low vacuum and Environmental SEM) to accommodate the widest range of samples of any SEM system. The motorized stage control and automation (x/y travel) allow the SEM to analyse high quantities of particles in unattended mode without any mechanically adjusting.

Results of the chemical measurements of the 12 elements as mentioned above are given as a relative content and translated into minerals using specific element abundances, absences, and ratios. The method was described by Leipe *et al.* (1999). The single particle X-ray microanalysis EDAX GENESIS 4000 includes an image analyzing program module, which identifies the diameter and the outline of the measured grain and calculates the perimeter, the area and a shape factor. The particle area (AREA) is evaluated by summing all the graphics pixels within the identified particle and using the pixels in x and y direction to convert the number of pixels to square micrometer. The average diameter (AVGDIA) is defined as the diameter of a circle with the same area (equation 1):

$$AVGDIA = \sqrt{\frac{4 \cdot AREA}{\pi}} \quad (1)$$

The perimeter (PERIM) is calculated using an empirical formula (equation 2):

$$PERIM = 2\sqrt{\pi} \cdot 0.886 \cdot \text{number_of_horizontal_segments} \cdot \sqrt{\frac{xFeret}{yFeret}} \quad (2)$$

where xFeret and yFeret are the length of the particle projections on x and y axes.

The shape factor characterizes the degree of roundness and is calculated following equation 3:

$$\text{shape} = 0.07958 \left(\frac{\text{perimeter}^2}{\text{area}} \right) \quad (3)$$

To describe the grain size and the sorting of the grain distribution, the logarithmic phi-scale is used (Folk 1974, equation 4).

$$\phi = -\log_2 \left(\frac{d}{1\text{mm}} \right) \quad (4)$$

where ϕ is the phi size, and d is the metric grain diameter.

These data were processed using the statistical program package SPSS and Microsoft Excel to characterize the morphometric data from the sediment, and the foraminifer respectively.

RESULTS

Multielement mapping, sample “nodulina 1”

Using the scanning electron microscope, spectral images of the following elements were created: Al, Ca, Fe, K, Mg, Mn, Na, P, S, Si, and Ti. Scatterplots of pixel intensities for all element pairs were investigated for clusters of intensity data. The scatterplots were subdivided into subregions with specific intensity thresholds and intensity ratios aiming at separation of the different clusters. According to specific element abundances, absences, and ratios, the following minerals could be discerned: albite, anorthite, apatite, ilmenite, orthoclase, plagioclase, pyrite, quartz, rutile, and titanite (Table 1, Fig. 2b). Furthermore, two different heavy minerals are found (presumably garnet and hornblende). Spaces between larger mineral grains are filled with clay particles, which could not be further determined due to their small size below the resolution of the spectral imaging system. Clay particles are also attached to the surface of larger grains, especially to quartz/opal and feldspar. It is difficult to distinguish the clay on feldspars due to some overlap in their element combination.

When the data of a certain pixel of all investigated elements could be assigned to a mineral, that pixel was given a certain color hue (or gray, when the element combination did not belong to the selected elements). Because the spatial resolution of

Table 1

Comparison between the surface coverage of identified minerals in the geochemical mapped surface of *N. dentaliniformis* (sample “nodulina 1”, second column), and the calculated relative grain areas of selected minerals of the sample “nodulina 2” (third column) and “substrate” (fourth column). Note that 100% in the third and fourth column are all as minerals identified grains in the sample

Mineral	% Surface coverage sample “nodulina 1”	% Grain area sample “nodulina 2”	% Grain area sample “substrate”
Quartz/Opal	41.81	32.90	49.69
Orthoclase	7.40	10.42	17.47
Albite	1.80	4.83	0.00
Plagioclase	2.60	1.19	0.00
Anorthite	0.80	0.00	0.27
Ilmenite	0.30	-	-
Titanite	0.30	0.47	0.00
Rutile	0.00	-	-
Heavy mineral 1	0.04	-	-
Heavy mineral 2	2.90	-	-
Apatite	0.02	0.15	0.39
Clay particles	37.00	46.78	30.65
Pyrite	0.03	-	-
Organic remains	5.00	-	-

the spectral images is rather poor, the brightness was calculated from an image of secondary electrons (SE), which adds more detail to the picture (Fig. 2a).

Counting all pixels belonging to a certain mineral, the relative amounts of all minerals in the recognized part of the image were calculated (Table 1, Fig. 2b). It should be noted, that the percentages are relative surface coverages, not mass percents. The calculated numbers strongly depend on the investigated part of the sample surface. Some minerals are represented only by a very few grains, therefore their relative amounts are subjected to considerable statistical fluctuations.

Single particle analysis, samples “nodulina 2” and “substrate”

The single particle analysis instrument provides data of morphometrical (diameter, shape etc.) and chemical (selected elements) characteristics of the identified grains. The content of the elements Al, Ca, Fe, K, Mg, Mn, Na, P, S, Si, and Ti oxides was available for both samples in percent. More than 2700 grains were identified from the sample “nodulina 2”, and over 800 from the “substrate” sample. Minerals were discerned using specific abundances, ratio and absences of given ox-

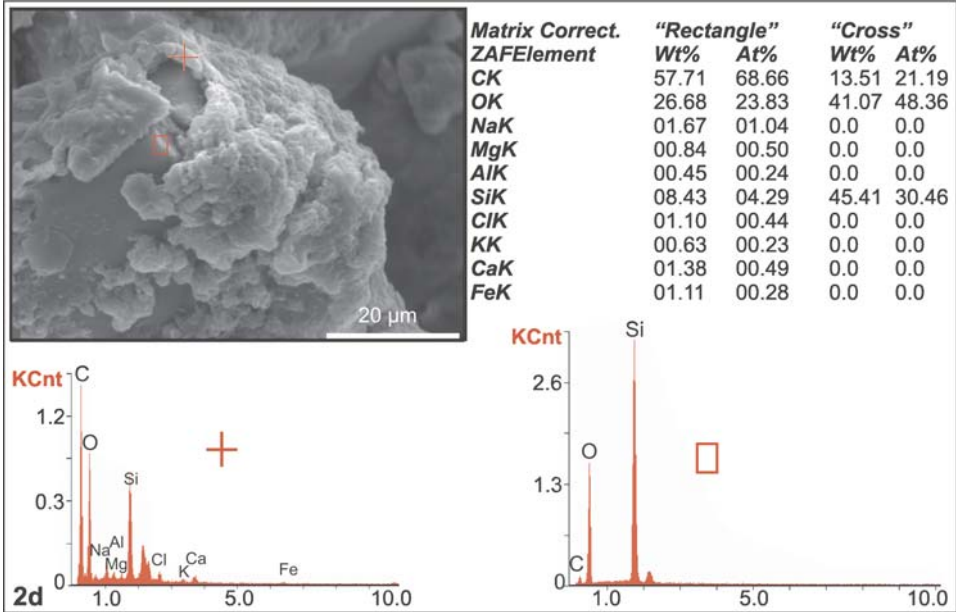
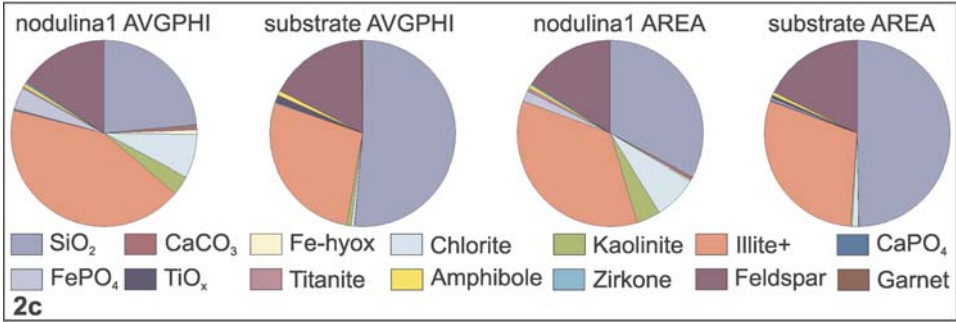
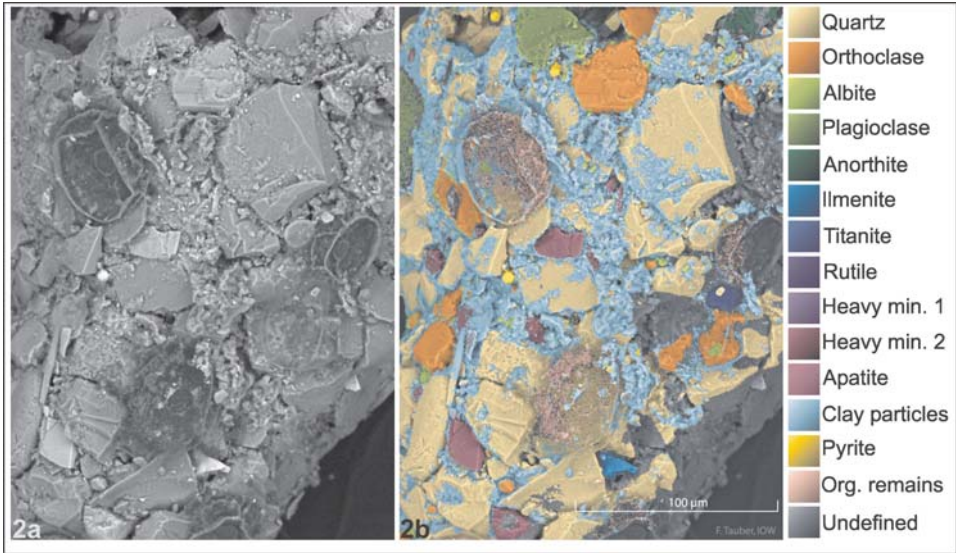


Table 2

Specific content of discerned minerals and mineral-complexes of the samples
“nodulina 2” and “substrate”

Mineral	nodulina 2 [%]	nodulina 2 [N]	nodulina 2 [% area]	substrate [%]	substrate [N]	substrate [% area]
SiO ₂	23.62	307	32.90	51.45	266	49.69
CaCO ₃	0.76	10	0.53	0	0	0
Fe-hyox	0.77	10	0.25	0	0	0
chlorite	7.62	99	7.43	0.58	3	0.93
kaolinite	3.38	44	4.08	0.77	4	0.40
illite+	42.69	555	35.27	27.47	142	29.32
CaPO ₄	0.23	3	0.15	0.19	1	0.39
FePO ₄	3.85	50	1.83	0.19	1	0.17
TiO _x	0.15	2	0.13	0.97	5	0.41
Titanite	0.23	3	0.47	0	0	0
Amphibole	0.69	9	0.70	0.97	5	0.60
Zirkone	0.23	3	0.11	0	0	0
Feldspar	15.69	204	16.12	17.21	89	17.74
Garnet	0.08	1	0.03	0.19	1	0.08

In the first column, minerals are listed: SiO₂ = crystalline and amorph mineral phases (quartz and opal), Fe-hyox = Iron oxides (magnetite, hematite), and hydroxides (limonite, goethite), illite+ = illite and mixed layered illite, TiO_x = rutile. In the second and fifth column (%), the content in percent grains is given. The third and sixth column [N] contain the absolute counting of the identified grains of the mineral and the fourth and eighth [% area] give the percentage of the area of the minerals in respect to the total area of identified mineral grains

←

Fig. 2. **a, b** – Detail of the ultimate chamber of *N. dentaliniformis* (SEM image), and results of the multielement mapping of the same area (b). All investigated elements are assigned to specific minerals. **c** – Diagrams of the mineral composition of samples “nodulina 2” and “substrate”, grain diameter in Φ -scale (AVGPHI) and the grain area (AREA). **d** – SEM image of a single grain broken off from a *N. dentaliniformis* shell, covered with an organic cement. Two measurements with the EDAX were carried out: The cross marks the point of the measurement of the organic cement (note the high content of carbon, and silicon), rectangle marks the EDAX measurement of the grain (quartz in this case). Beside the SEM picture, the detailed EDAX ZAF quantified and normalized values of the measured elements (listed as weight percent [Wt%] and atomic percent [At%])

ides. Table 2 gives an overview on the identified minerals, their content in percent and the percentage of their area.

To find out the degree of similarity, the Pearson's correlation coefficient (equation 5), was calculated. It measures the strength of the linear relationship between two variables X and Y, and can take the values from -1.0 to 1.0 . Where -1.0 is a perfect negative (inverse) correlation, 0.0 is no correlation, and 1.0 is a perfect positive correlation.

$$\rho_{xy} = \frac{COV(X,Y)}{\sqrt{V(X)}\sqrt{V(Y)}} = \frac{\sum_{i=1}^n (x_i - \bar{x})(y_i - \bar{y})}{\sqrt{\sum_{i=1}^n (x_i - \bar{x})^2} \sqrt{\sum_{i=1}^n (y_i - \bar{y})^2}} \quad (5)$$

where COV = covariance and V = variance.

For the calculated Pearson's correlation coefficient, the significance level for correlation characterizes the probability of a linear dependency between the two variables. The value 0.0 is a perfect linear dependence, the value 1.0 a perfect non-linearly dependency. The significance level for correlation (t) is calculated following equation 6, where ρ = the Pearson's correlation coefficient and N the number of observations.

$$t = \rho \sqrt{\frac{N-2}{1-\rho^2}} \quad (6)$$

The Pearson's correlation coefficient (r) for the proportional surface coverage of all identified mineral grains of the selected eight minerals quartz and skeletal opal (SiO_2), orthoclase, albite, plagioclase, anorthite, titanite, apatite and clay minerals (see Table 1) of the samples "nodulina 1" and "nodulina 2" is 0.96 ($t = 0.00$). It is 0.96 ($t = 0.00$) between the samples "nodulina 1" and "substrate", and 0.87 ($t = 0.00$) between the samples "nodulina 2" and "substrate". This result points to a very similar composition of all the three samples in their mineralogical (chemical) composition.

If the percentage of counting of all 14 identified mineral grains in the samples "nodulina 2" and substrate is taken into account, the correlation has also a high grade ($r = 0.80$; $t = 0.0$). The ρ is much higher, when the index is calculated for the area $\rho = 0.94$; $t = 0.0$). In these samples, only the SiO_2 (quartz and opal) content of the sediment is higher in respect to the "nodulina 2" sample (Fig. 2c).

The results of the grain size and shape characterizing statistics are very different from the former data of the mineral composition (Figs 2c, 3 and Table 3). There is no distinct correlation between the sediment and the foraminifer. The Pearson correlation coefficient between the grain size [Φ -scale] of the samples "nodulina 2" and "substrate" is -0.01 ($t = 0.86$). Between the areas of the grains of the two samples, ρ is 0.01 ($t = 0.72$), between the perimeters, ρ is -0.01 ($t = 0.78$), and for the shapes -0.02 ($t = 0.51$).

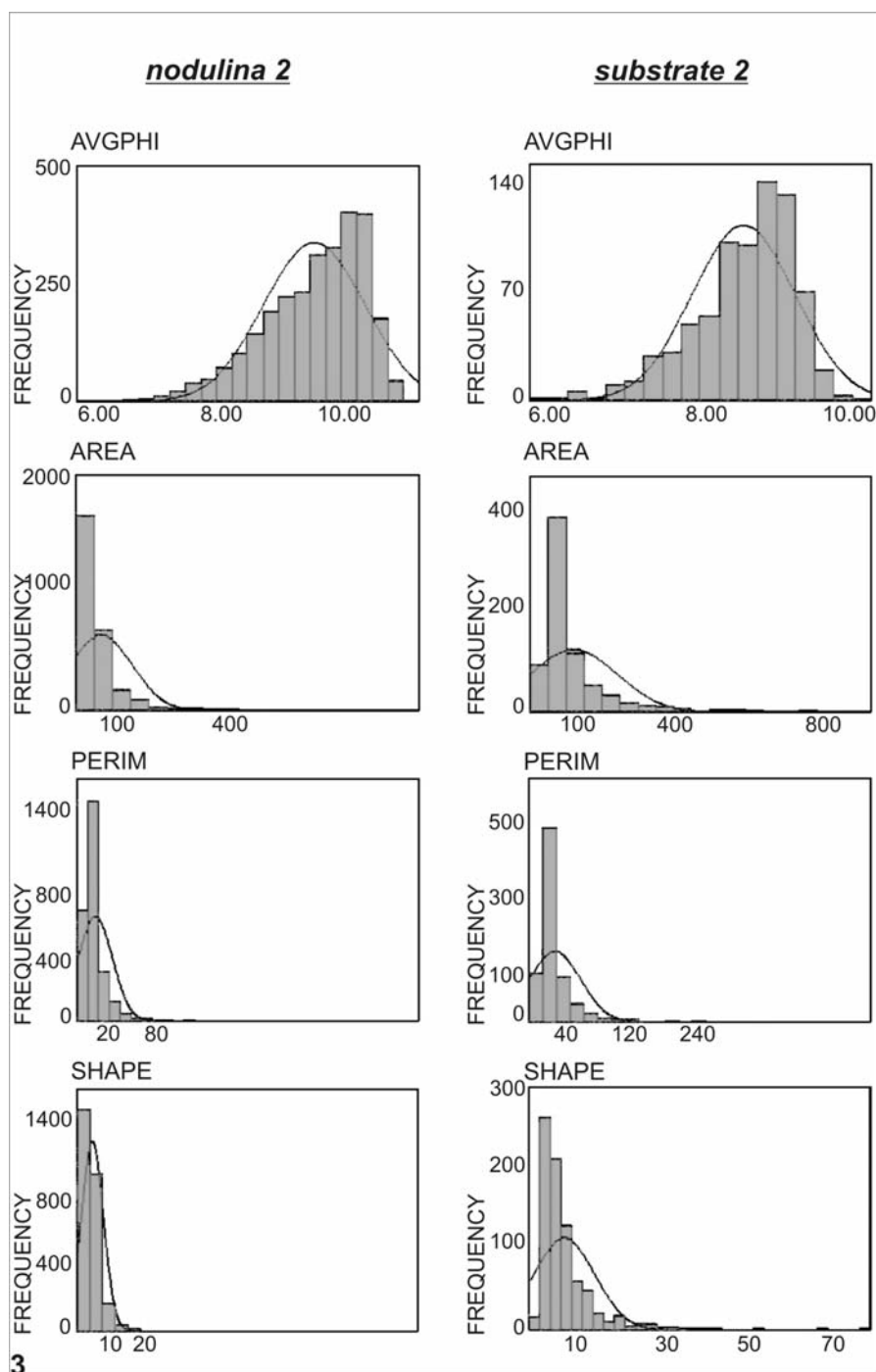


Fig. 3. Histograms of the morphometric analysis of samples “nodulina 2” and “substrate”. AVGPHI = average grain diameter, Φ -scale, AREA = grain area, PERIM = grain perimeter, and SHAPE = grain shape. For the algorithms, please refer to the text

Table 3

Grain-size, area, perimeter and shape statistics of the samples “nodulina 2” and “substrate”

	nodulina 2					substrate				
	DIAM	PHI	AREA	PERIM	SHAPE	DIAM	PHI	AREA	PERIM	SHAPE
counted grains	2757	2757	2757	2757	2757	805	805	805	805	805
mean	2.06	9.20	45.48	12.05	3.54	3.26	8.45	97.05	28.55	7.07
median	1.53	9.35	18.30	7.63	2.33	2.58	8.60	51.95	17.66	5.04
standard dev	1.62	0.81	85.56	15.86	4.37	2.07	0.68	120.99	37.02	7.07
skewness	3.82	-0.86	4.48	7.60	11.72	3.09	-0.98	3.24	6.04	3.75
minimum	0.63	5.48	0.31	2.91	0.80	1.00	5.66	0.78	6.19	1.07
maximum	22.33	10.63	915.04	314.51	129.61	19.75	9.97	922.61	472.04	77.40
range	21.70	5.15	914.74	311.60	128.81	18.75	5.66	921.83	465.85	76.33

DIAM = average diameter [μm], PHI = diameter, calculated in the Φ -scale, AREA = calculated area of the grain [μm^2], PERIM = calculated perimeter of the grain [μm], SHAPE = calculated shape-factor

Table 4

Grain-size, area, perimeter and shape statistics of SiO_2 -grains of the samples “nodulina 2” and “substrate”

SiO_2	nodulina 2				substrate			
	PHI	AREA	PERIM	SHAPE	PHI	AREA	PERIM	SHAPE
counted grains	307	307	307	307	266	266	266	266
mean	8.86	65.76	10.94	1.96	8.41	99.15	28.01	6.18
median	8.87	35.28	7.90	1.35	8.52	58.13	16.23	4.15
standard dev	0.78	101.35	10.99	2.62	0.67	120.89	38.29	6.46
skewness	-0.34	4.43	3.96	8.762	-1.14	3.14	5.10	2.86
minimum	6.53	0.48	2.91	0.91	5.66	14.24	6.38	1.11
maximum	10.32	915.04	84.59	36.15	9.53	751.85	374.41	42.53
range	4.00	914.56	81.68	35.24	3.87	737.61	368.03	41.42

PHI = diameter, calculated in the Φ -scale, AREA = calculated area of the grain [μm^2], PERIM = calculated perimeter of the grain [μm], SHAPE = calculated shape-factor

Table 5

Pearson's correlation index (ρ) and, in paranthesis, level of significance (t), between the samples "nodulina 2" and "substrate" for SiO₂ and feldspar

	nodulina 2 - substrate SiO ₂	nodulina 2 - substrate feldspar
Pearson's correlation index PHI	-0.073 (0.670)	0.900 (0.002)
Pearson's correlation index PERI	-0.048 (0.783)	0.838 (0.009)
Pearson's correlation index SHAPE	-0.003 (0.985)	-0.268 (0.521)
Pearson's correlation index AREA	0.018 (0.915]	0.784 (0.021)

Table 6

Grain-size, area, perimeter and shape statistics of feldspar-grains of the samples "nodulina 2" and "substrate"

feldspar	nodulina 2				substrate			
	PHI	AREA	PERIM	SHAPE	PHI	AREA	PERIM	SHAPE
counted grains	204	204	204	204	89	89	89	89
mean	9.09	48.49	10.60	2.27	8.40	105.23	33.54	8.49
median	9.00	23.17	6.73	1.51	9.00	57.12	20.99	5.66
st. deviation	0.87	70.24	12.68	2.04	0.82	137.98	47.03	9.00
skewness	-0.68	2.77	6.70	3.62	-0.75	3.24	5.85	4.10
minimum	6.00	0.46	2.91	0.93	6.00	11.10	6.66	1.31
maximum	10.00	379.25	144.50	16.66	10.00	788.12	401.32	67.36
range	4.00	378.79	141.59	15.73	4.00	777.02	394.66	66.05

PHI = diameter, calculated in the Φ -scale, AREA = calculated area of the grain [μm^2], PERIM = calculated perimeter of the grain [μm], SHAPE = calculated shape-factor.

If the main coarse-grained components, SiO₂ and feldspar of the foraminiferal shell (sample "nodulina 2") and the ambient sediment (sample "substrate") are taken into account, there are no correlations for the SiO₂. The feldspar grains show medium to good correlations for the diameter, perimeter and area and no correlation for the shape (Tables 4–6).

The range of the grain size with a minimum of 0.63 μm and a maximum of 22.33 μm is much larger for the foraminifer compared with that of the substrate with a minimum of 5.66 μm and 9.53 μm . All measured grains are moderately sorted (standard deviation [Φ -scale] = 0.5–1).

DISCUSSION

The chemical analysis, measurements and calculations of grain characteristics of the studied agglutinated foraminifer *N. dentaliniformis* give substantial insight into the mode of shell formation. In terms of the selection of specific minerals for shell construction, it could be clearly shown that this foraminifer species does not select for any minerals. The calculated Pearson's correlation coefficient gives a high grade of correspondence between the shell composition and the ambient sediment.

The possible redeposition of the shell is excluded due to the infaunal mode of life of this foraminifer and the selection of living specimens (Lutze, 1964, 1965). The results of the chemical scanning of the last chambers surface correlate well with the sediment composition.

There was no or low grade correlation between single grain physical characteristics of the foraminiferal shell and the sediment. This fact points to the hypothesis that this species is selective for grains, specific in size and shape. The investigation of SiO₂ (quartz and opal) and feldspar, which is the coarser grain fraction of the shell, gives weight to the hypothesis that this foraminifer is selective for grains, specific in size and shape (Tables 4–6). The shape modulus of samples “nodulina 2” versus “substrate” is 1.11/2.15 for SiO₂ and 1.19/1.69 for feldspar. The higher the shape factor, the higher is the complexity of the outline of the grain. This means that *N. dentaliniformis* is selective in its coarse fraction for bigger, rounded grains for very fine minerals and in the fine-grained fraction, building the gussets and between the bigger grains. The enhanced content of fine fraction could not be explained with the preparation technique, especially with the intense treatment with H₂O₂ (Allen & Thornley, 2004).

It should be determined, whether or not the non-correlation between the investigated sediment and the foraminiferal shell might be an effect of the inhabited microhabitat, which may differ in its grain-size distribution from the homogenized “substrate” sample. Some of the SiO₂, detected in the single particles, may well be a component of the organic cement, possibly produced by the foraminifer itself (Fig. 2d). The origin of the SiO₂ which was evident in the investigated cement should be investigated further.

Future work will concentrate on systematic investigations of larger quantities of agglutinated foraminifers and the sediment of their microhabitats, using refined sampling techniques.

CONCLUSION

High resolution Single Particle Analysis by scanning electron microscopy and X-ray microanalysis is introduced as a new technique to investigate tests of agglutinated foraminifers. Multielement surface scanning as well as the chemical and grain size and shape analysis of single grains of a foraminiferal test and the ambient sediment have clearly shown that this method is a suitable tool to investigate the shell composition of agglutinated foraminifers and their mode of shell construction.

For *N. dentaliniformis* it could be shown that this species is not selective for specific minerals, but for grains that are specific in size and shape.

Acknowledgements

We thank the Institute of Baltic Sea Research Warnemünde for the opportunity to use the technical facilities for this study. Aspects of this study were supported by the University of Bonn. The authors are grateful to Drs M. Kusiak and J. Tyszka (Kraków) for their valuable suggestions and comments. We thank Dr M. A. Kaminski (London) for the final review of the manuscript, and Prof. M. Langer (Bonn) for insightful discussions. The first author was supported by the German Science Foundation (DFG), the third author was supported with a sponsorship by the DBU (German Federal Environmental Foundation) within the focus “The southern Baltic Sea and its coasts in change”.

REFERENCES

- Allen, K., Roberts, S. & Murray, J. W., 1998. Fractal grain distribution in agglutinated foraminifera. *Paleobiology*, 24 (3): 349–358.
- Allen, K., Roberts, S. & Murray, J. W., 1999. Marginal marine agglutinated foraminifera: Affinities for mineral phases. *Journal of Micropaleontology*, 18: 183–191.
- Allen, J. R. L. & Thornley, D. M., 2004. Laser granulometry of Holocene estuarine silts: effects of hydrogen peroxide treatment. *The Holocene*, 14 (2): 290–295.
- Bender, H. & Hemleben, C., 1995. Test structure and classification in agglutinated foraminifera. In: Kaminski, M. A., Geroch, S. & Gasiński, M. A. (eds), Proceedings of the Fourth International Workshop on Agglutinated Foraminifera. *Grzybowski Foundation Special Publication*, 3: 27–70.
- Brady, H. D., 1881. Notes on some of the reticularian Rhizopoda of the Challenger Expedition. Part III.1. Classification. 2. Further notes on new species. 3. Note on *Biloculina* mud. *Quarterly Journal of Microscopical Science. New Series*, 21: 31–71.
- Folk, R. L., 1974. *The petrology of sedimentary rocks*. Austin, Tex., Hemphill Publishing Co., 182 pp.
- Hermelin, J. O. R., 1987. Distribution of Holocene benthic foraminifera in the Baltic Sea. *Journal of Foraminiferal Research*, 17 (1): 62–73.
- Kuhnt, W., Moullade, M. & Kaminski, M. A., 1996. Ecological structuring and evolution of deep-sea agglutinated foraminifera. *Revue de Micropaléontologie*, 39 (4): 271–281.
- Leipe, T., Löffler, A., Bahlo, R. & Zahn, W., 1999. Automatisierte Partikelanalyse von Gewässerproben mittels Raster-Elektronenmikroskopie und Röntgen-Mikroanalytik. *Vom Wasser*, 93: 21–37.
- Loeblich, A. R. & Tappan, H. 1989. Implications of wall composition and structure in agglutinated foraminifer. *Journal of Paleontology*, 63 (6): 769–777.
- Lutze, G. F., 1964. Zum Färben rezenter Foraminiferen. *Meyniana*, 14: 43–47.
- Lutze, G. F., 1965. Zur Foraminiferen-Fauna der Ostsee. *Meyniana*, 15: 75–142.
- Mancin, N., 2001. Agglutinated foraminifera from the Epiligurian succession (Middle Eocene/Lower Miocene, Northern Apennines, Italy): Scanning electron microscopic characterization and paleoenvironmental implications. *Journal of Foraminiferal Research*, 31 (4): 294–308.
- Nomura, R., 1988. Ecological significance of wall microstructure of benthic foraminifera in the southwestern Sea of Japan. *Revue de Paléobiologie, Volume Special*, 2 (Benthos '86): 859–871.